Dalton Transactions

Cite this: *Dalton Trans.*, 2011, **40**, 12479

www.rsc.org/dalton

PAPER

New group 11 complexes with metal–selenium bonds of methyldiphenylphosphane selenide: a solid state, solution and theoretical investigation†

Alexandra Pop,[a] Anca Silvestru,*[a] M. Concepción Gimeno,[b] Antonio Laguna,[b] Monika Kulcsar,[b] Massimiliano Arca,[c] Vito Lippolis*[c] and Anna Pintus[c]

Received 3rd July 2011, Accepted 2nd September 2011
DOI: 10.1039/c1dt11268f

Reactions between methyldiphenylphosphane selenide, $SePPh_2Me$, and different group 11 metal starting materials {CuCl, $[CuNO_3(PPh_3)_2]$, AgOTf, $[AgOTf(PPh_3)]$ ($OTf = OSO_2CF_3$), [AuCl(tht)], $[Au(C_6F_5)(tht)]$ and $[Au(C_6F_5)_3(tht)]$ (tht = tetrahydrothiophene)} were performed in order to obtain several new species with metal–selenium bonds. The new complexes $[CuCl(SePPh_2Me)]$ (**1**), $[AgOTf(SePPh_2Me)]$ (**2**), $[AuCl(SePPh_2Me)]$ (**5**), $[Au(C_6F_5)(SePPh_2Me)]$ (**6**) and $[Au(C_6F_5)_3(SePPh_2Me)]$ (**7**) were isolated and structurally characterized in solution by multinuclear NMR spectroscopy (^1H, ^{31}P, ^{77}Se and ^{19}F where appropriate). Solid products were isolated also from the reactions between $SePPh_2Me$ and $[CuNO_3(PPh_3)_2]$ or $[AgOTf(PPh_3)]$, respectively. NMR experiments, including low temperature ^1H and ^{31}P NMR, revealed for them a dynamic behaviour in solution, involving the transfer of selenium from PPh_2Me to PPh_3. In case of the isolated silver(I) containing solid an equilibrium between, respectively, monomeric $[AgOTf(PPh_3)(SePPh_2Me)]$ (**3**) and $[AgOTf(PPh_2Me)(SePPh_3)]$ (**4**), and dimeric $[Ag(PPh_3)(\mu\text{-}SePPh_2Me)]_2(OTf)_2$ (**3a**) and $[Ag(PPh_2Me)(\mu\text{-}SePPh_3)]_2(OTf)_2$ (**4a**) species was observed in solution. In case of the isolated copper(I) containing solid the NMR studies brought no clear evidence for a similar behaviour, but it can not be excluded in a first stage of the reaction. However the transfer of selenium between the two triorganophosphanes takes place also in this case, but the NMR spectra suggest that the final reaction mixture contains the free triorganophospane selenides $SePPh_2Me$ and $SePPh_3$ as well as the complex species $[CuNO_3(PPh_3)_2]$, $[CuNO_3(PPh_2Me)_2]$ and $[CuNO_3(PPh_3)(PPh_2Me)]$ in equilibrium. Single-crystal X-ray diffraction studies revealed monomeric structures for the gold(I) **6** and gold(III) **7** complexes. In case of compound **6** weak aurophilic gold(I) $\cdots$ gold(I) contacts were also observed in the crystal. DFT calculations were performed in order to understand the solution behaviour of the silver(I) and copper(I) species containing both P(III) and P(V) ligands, to verify the stability of possible dimeric species and to account for the aurophilic interactions found for **6**. In addition, the nature of the electronic transitions involved in the absorption/emission processes observed for **6** and **7** in the solid state were also investigated by means of TD-DFT calculations.

Introduction

Triorganophosphane chalcogenides (Se, Te) have attracted much interest in recent years due to their ability to form complexes with metal–chalcogen bonds,[1–12] which are promising candidates as precursors for semiconductors.[3–6] The soft chalcogen and the polar phosphorus–chalcogen bond make them suitable to coordinate soft metal centres.

Several studies were reported in recent years related to metal complexes of triorganophosphane chalcogenides. Few adducts of main group metals of type $[MX_3(EPR_3)]$ (M = Al; E = O, S, Se; X = Cl, Br,[7,8] M = Sb, E = O, S, Se; X = Cl, Br, I[13–17]) and $[SbCl_5(EPR_3)]$ (E = O, S, Se)[18] were described. Among the transition metal containing species only few triorganophosphane tellurides of tungsten, gold, silver and copper were either

[a]*Faculty of Chemistry and Chemical Engineering, "Babes-Bolyai" University, RO-400028, Cluj-Napoca, Romania. E-mail: ancas@chem.ubbcluj.ro; Fax: 0040 264 590818; Tel: 0040 264 593833*
[b]*Departamento de Química Inorgánica, Instituto de Síntesis Química y Catálisis Homogénea, Universidad de Zaragoza-C.S.I.C, E-50009, Zaragoza, Spain*
[c]*Dipartimento di Chimica Inorganica ed Analitica, Università degli Studi di Cagliari, S.S. 554 Bivio per Sestu, 09042, Monserrato (CA), Italy*

† Electronic supplementary information (ESI) available: X-ray crystallographic data in CIF format for **6** and **7**; Figures S1–S3 contain NMR spectra revealing the solution behaviour of the solid species isolated in reactions (*iii*) and (*vii*); Tables S1–S6 report the optimized geometries for complexes **3**, **3a**, **6**, **6′**, **7** and **8**; Tables S7–S9 summarise the main electronic transitions calculated at TD-DFT level for **6**, **6′**, and **7**. CCDC reference numbers 827811 and 827812. For ESI and crystallographic data in CIF or other electronic format see DOI: 10.1039/c1dt11268f

investigated in solution or isolated and structurally characterized as short living species.[1,9] In the presence of Lewis acids or free phosphanes such metal complexes are kinetically labile and suffer decomposition, depositing chalcogen and forming a more stable triorganophosphane complex. Such a behaviour was observed for $[MCl(TePR_3)]$ complexes (R = Pr^i, M = Cu, Au, Ag; R = Bu^t, M = Ag).[19] Dimeric or polymeric associations were found in $[Ag_2(NMs_2)_2(TePPr^i_3)_2]$, $[Ag_2(NMs_2)(TePPr^i_3)_4]^+[NMs_2]^-\cdot CH_3CN$ (NMs = dimethylsulfonylamide) and $[Ag(EPPr^i_3)_2]^+[SbF_6]^-$ (E = Se, Te), respectively.[19] Several group 11 complexes were described with the flexible 1,1′-bis(diphenylselenophosphoryl)ferrocene ligand which was found to act as bridging or *trans* chelating moiety.[20–22] Ligands of type $Ph_2P(Se)(CH_2)_nP(Se)Ph_2$ act as bridging units towards copper or gold, involving either both chalcogen atoms or only one of them in metal coordination.[23–27]

We report here on the synthesis and spectroscopic characterization of several new group 11 complexes with the neutral ligand $SePPh_2Me$. A deeper understanding of the coordination chemistry of triorganophosphane selenides towards coinage metal ions (Cu, Ag, Au) can open to future applications of the related complexes featuring Cu–, Ag–, or Au–chalcogen bonds, which to date are rather uncommon and not easy to handle.

Results and discussion

Synthesis

The triorganophosphane selenide ligand $SePPh_2Me$ was reacted in a 1 : 1 molar ratio with the appropriate group 11 metal containing starting material as depicted in Scheme 1.

With the exception of compound **5** which was isolated as a brownish oil, all the other species described in this paper are crystalline solids (colourless – species **1–4** and **7**, or pale yellow compound **6**).

Spectroscopic characterization

^1H and ^{31}P NMR data for the complexes containing only one type of organophosphorus ligand ($SePPh_2Me$, *i.e.* compounds **1**, **2**, **5–7**) suggest the existence of only one species in solution, while for the complexes containing more than one type of organophosphorus ligands the NMR spectra suggest a dynamic behaviour. However, for the phenyl and the methyl groups attached to phosphorus the ^1H NMR spectra exhibit resonances with the expected pattern due to the proton-proton and phosphorus-proton couplings, respectively. The ^{31}P NMR spectra of the complexes **1**, **2** and **5–7** exhibit singlet resonances corresponding to the $SePPh_2Me$ moiety, with characteristic ^{77}Se and ^{13}C satellites, (δ 21.17 for **1**, 23.1 for **5**, 24.2 for **6** and 26.05 ppm for **7**, respectively, in $CDCl_3$ solutions and 27.7 ppm for **2** in acetone-d_6). A significant decrease of the ^1J(SeP) coupling constant was observed in all these species (range 535.4–598.5 Hz) in comparison with the free ligand $SePPh_2Me$ [δ 23.24 ppm, ^1J(SeP) 717.3 Hz, in $CDCl_3$ and δ 23.26 ppm, ^1J(SeP) 733.8 Hz in acetone-d_6].

In case of the gold complexes **6** and **7** the ^{19}F NMR spectra contain three resonances with the expected patterns for the C_6F_5 groups. In case of the square-planar compound **7** the three C_6F_5 groups attached to gold give two different ^{19}F sets of resonances in a 1 : 2 molar ratio for the non-equivalent C_6F_5 groups (one of them *trans* to selenium and the other two *trans* each other, respectively).

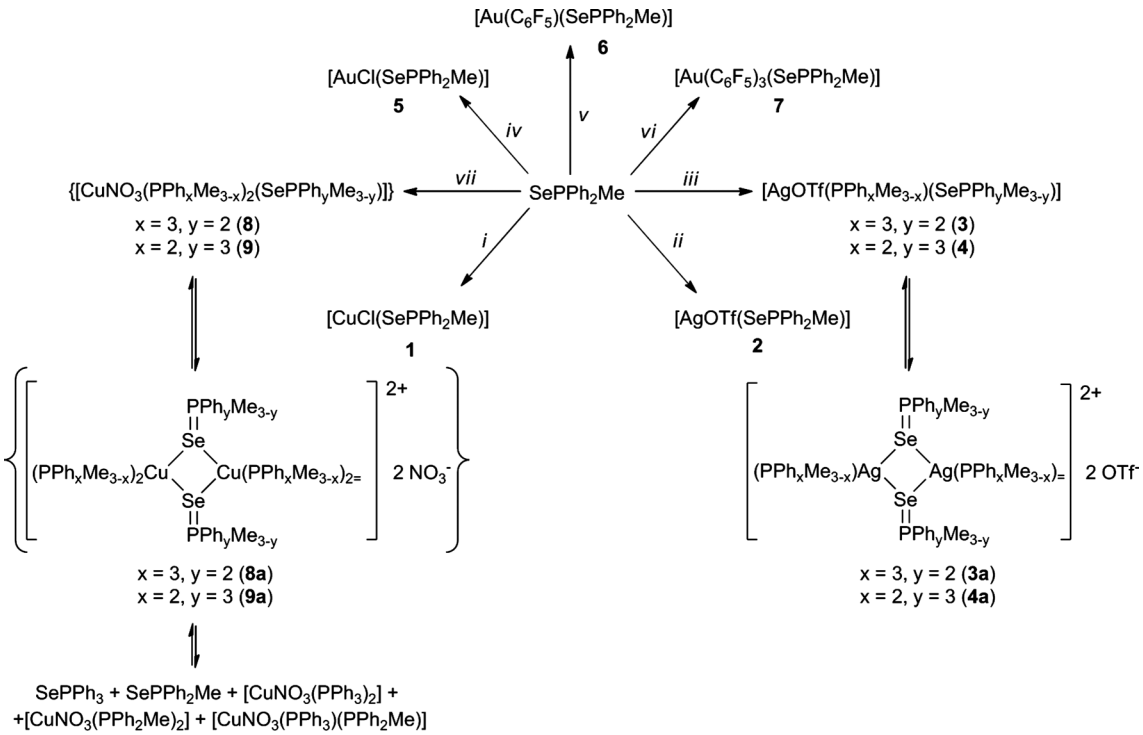

(i) CuCl, CH_2Cl_2; *(ii)* AgOTf, CH_2Cl_2; *(iii)* [AgOTf(PPh_3)], acetone; *(iv)* [AuCl(tht)], CH_2Cl_2; *(v)* [Au(C_6F_5)(tht)], CH_2Cl_2; *(vi)* [Au(C_6F_5)$_3$(tht)], CH_2Cl_2; *(vii)* [$CuNO_3(PPh_3)_2$], CH_2Cl_2;

Scheme 1

The ESI+ MS spectrum of compound **1** revealed two peaks at *m/z* 720.8 (10%, $[(CuSePPh_2Me)_2Cl^+]$) and at *m/z* 622.7 (100%, $[Cu(SePPh_2Me)_2^+ + H]$), while the ESI− MS spectrum presents a peak at *m/z* 613.7 (100%), corresponding to the $[Cu(PPh_2Me)(SePPh_2Me)Cl_2^-]$ species. The silver complex **2** presents in the ESI+ spectrum a peak at *m/z* 559.4 (100%, $[M^+ + Na]$) and in the ESI− spectrum a peak at *m/z* 406.7 corresponding to the anion $[Ag(OTf)_2^-]$.

This behaviour suggests in case of compounds **1** and **2** the existence of only one species in solution, at least at room temperature, either monomeric (Scheme 2, **a**), or dimeric with either selenium (Scheme 2, **b**) or an anionic ligand (Cl^- or OTf^-) (Scheme 2, **c**) bridging moieties, but with equivalent $SePPh_2Me$ ligands.

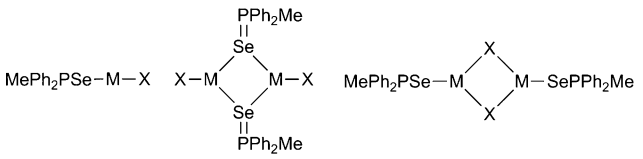

Scheme 2

The room temperature ^{31}P NMR spectra of the solid products isolated from reactions (*iii*) and (*vii*) (Scheme 1), respectively, both in $CDCl_3$ or acetone-d_6 solution, show four different resonances, two of them sharp, accompanied by ^{77}Se satellites, corresponding to the *P*(V)═Se moieties and the other two broad, belonging to *P*(III) environments (See ESI Fig. S1†). At a first glance, this pattern suggest an equillibrium mixture of two species in each case, containing both phosphorus(III) and phosphorus(V) ligands.

Solution behaviour of the silver(I) species of type $\{[Ag(PPh_xMe_{3-x})(SePPh_yMe_{3-y})]OTf\}_n$

In case of the solid product isolated from reaction (*iii*) (Scheme 1) the ^1H NMR spectrum (acetone-d_6) shows in the aliphatic region two resonances (δ 1.85 ppm, $^2J_{PH}$ 5.9 Hz and δ 2.60 ppm, $^2J_{PH}$ 13.6 Hz). The observed coupling constants are in accordance with the presence of both a P(III) and a P(V) species containing P*Me* protons. Taking in account these results and the fact that for phosphine complexes of coinage metals a dynamic behaviour in solution, involving either M–PPh_3 and/or S–$MPPh_3$ bond dissociation, is well known,[28–31] low temperature NMR experiments were performed (Fig. 1), both for the isolated solid product and for a 1 : 1 : 1 reaction mixture of PPh_3 + AgOTf + $SePPh_2Me$ realized directly in the NMR tube. We obtained the same spectra in both cases. While the ^{31}P resonances assigned to the P═Se moieties remained almost unchanged with the temperature variation, the resonances assigned to $Ag(PPh_3)$ (δ 10.5 ppm, broad) and $Ag(PPh_2Me)$ (δ −7.3 ppm, broad), in acetone-d_6, changed according to an equilibrium between dimeric and monomeric species, as depicted in Scheme 1.

At −60 °C, instead of the large resonance at δ 10.5 ppm, two resonances were observed, with a pattern of doublet of doublets each of them falling at δ 8.61 and 9.64 ppm, respectively. This pattern is determined by the $^{107}Ag–^{31}P$ and $^{109}Ag–^{31}P$ couplings. In case of the discussed silver species the observed coupling constants are: δ 8.61 ppm [$^1J(^{107}Ag–^{31}P)$ 618.9 Hz, $^1J(^{109}Ag–^{31}P)$ 539.6 Hz]

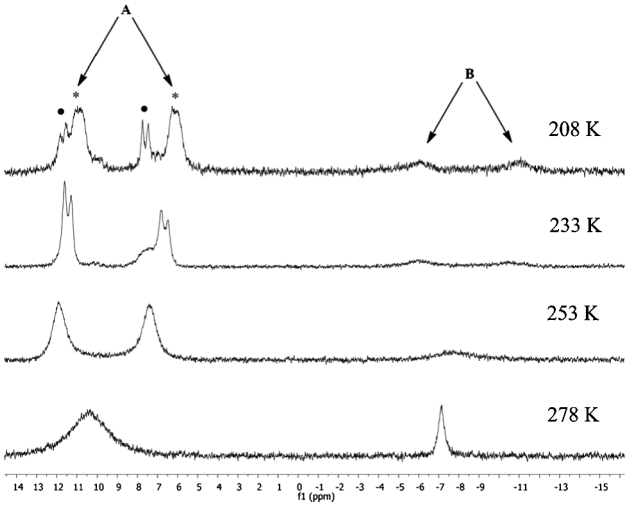

Fig. 1 VT ^{31}P NMR spectra (−15 ÷ +14 ppm region) of species **3** (**A**, *) and **3a** (A, ·) and **4** and **4a** (B), respectively.

and δ 9.64 ppm [$^1J(^{107}Ag–^{31}P)$ 526.3 Hz, $^1J(^{109}Ag–^{31}P)$ 460.8 Hz], and they correspond to the monomeric **3** and the dimeric **3a** species (Scheme 1), respectively. In accordance with the previously reported observation that the $^1J(^{107}Ag–^{31}P)$ coupling constants increase with decreasing of the Ag–P distance[32] and that they are inversely proportional with the coordination number of the silver atom,[31] the resonance at δ 8.61 ppm could be assigned to a monomeric species containing a dicoordinate silver atom, while the resonance at δ 9.64 ppm could be assigned to a dimeric species containing a tricoordinate silver atom. The second broad resonance (δ −7.3 ppm at room temperature) gives rise at low temperature to a broad doublet [at −60 °C δ −8.48 ppm, ^1J(Ag–P) 594.8 Hz]. For the species **4** and **4a** (Scheme 1) we presume a similar behaviour with that one described before for species **3** and **3a** (Scheme 1), but the corresponding resonances are not well resolved in this case. A further lowering of the temperature did not result in a better separation of the resonances. By contrast, a broadening in the base line of these resonances was observed. Using the Eyring relation[33] we determined at the coalescence temperature T_c = 5 °C a medium value for the free enthalpy $\Delta G^{\#}$ of 15.21 kcal mol^{-1} for the equilibrium process between the monomeric **3** and the dimeric **3a** species depicted in Scheme 1. According to the intensity of the resonances, the monomeric species is predominant in solution at low temperature. Similarly, for the equilibrium related to the monomeric $[Ag(PPh_2Me)(SePPh_3)]^+$ (**4**) and the dimeric $[Ag(PPh_2Me)(SePPh_3)]_2^{2+}$ (**4a**) species a medium value for the free enthalpy $\Delta G^{\#}$ of 11.96 kcal mol^{-1} was calculated at the coalescence temperature T_c = −20 °C from the ^{31}P NMR data.

The aliphatic region of the ^1H NMR spectra changed at low temperature to two broad resonances for the PPh_2Me and $SePPh_2Me$ protons, respectively (see ESI, Fig. S2†). The ^1H NMR resonances at low temperature, even for the methyl groups attached to phosphorus in the two species, undergo a behaviour consistent with a very slow rotation of the organic groups around the Se–Ag and P–Ag bonds, respectively, the well defined doublet resonances in the aliphatic region at room temperature become very large, broad singlet signals at low temperature.

A coordination pattern of the triorganophosphane chalcogenide ligand with the chalcogen atom bridging two metal centres

Table 1 NMR data for starting materials and complexes involving Ag(I) and Cu(I) species

acetone-d_6			$CDCl_3$		
Compound	δ^{31}P [ppm]	$^1J_{SeP}$ [Hz]	Compound	δ^{31}P [ppm]	$^1J_{SeP}$ [Hz]
PPh_3	–5.81s		PPh_3	–6.0s	
PPh_2Me			PPh_2Me	–26.84s	
$SePPh_3$	35.14s	747.2	$SePPh_3$	35.5s	738
$SePPh_2Me$	23.6s	733.8	$SePPh_2Me$	23.24s	717.3
$[AgOTf(PPh_3)]$	12.53d, br.		$[CuNO_3(PPh_3)_2]$	–1.87, br.	
$[AgOTf(SePPh_2Me)]$ (**2**)	27.7s	535.4	$[CuCl(SePPh_2Me)]$ (**1**)	21.17s	598.5
$[AgOTf(PPh_3)]$ + $SePPh_2Me$ (solid product-reaction (*iii*), RT)			**$[CuNO_3(PPh_3)_2]$ + $SePPh_2Me$** (solid product-reaction (*vii*), RT)		
$[AgOTf(PPh_3)(SePPh_2Me)]$ (**3**) +	10.5s		$[CuNO_3(PPh_2Me)_2]$	–17.4s, br.	
$[Ag(PPh_3)(\mu\text{-}SePPh_2Me)]_2(OTf)_2$ (**3a**)	25.8s	595.4	$[CuNO_3(PPh_3)_2]$	–1.2s, br.	
			$[CuNO_3(PPh_3)(PPh_2Me)]$		
$[AgOTf(PPh_2Me)(SePPh_3)]$ (**4**) +	–7.3s, br.		$SePPh_2Me$	23.3s	715.3
$[Ag(PPh_2Me)(\mu\text{-}SePPh_3)]_2(OTf)_2$ (**4a**)	33.6s	625.0	$SePPh_3$	35.4s	728.0
PPh_3 + AgOTf + $SePPh_2Me$	10.3s, br.		**$[CuNO_3(PPh_3)_2]$ + $SePPh_2Me$**	–17.9s, br.	
(RT, NMR tube scale reaction)	25.8s	602.9	(RT, NMR tube scale reaction)	–1.4s, br.	
	–7.4s,br.			23.2s	715.5
	33.7s	629.4		35.3s	728.1
$SePPh_3$ + AgOTf (RT, NMR tube scale reaction)			**PPh_3 + $SePPh_2Me$** (RT, NMR tube scale reaction)		
$[AgOTf(SePPh_3)]$	38.3s	564.0	PPh_2Me	–23.0s, br.	
			PPh_3	–5.5s, br.	
			$SePPh_2Me$	23.2s	717.0
			$SePPh_3$	35.3s	728.8

was previously described in solid state for other sulfur, selenium or tellurium containing ionic species.[19,23,24,26,31]

The ^{19}F NMR spectrum of the solid product isolated from reaction (*iii*) exhibits only one singlet resonance (δ –78.5 ppm), close to the value found in the ^{19}F NMR spectrum of complex **2** (–79.8 ppm) and to that found for the ionic species $[Ag(PPh_3)(SCN_4Me)]_2(OTf)_2$ (–77.9 ppm).[31] The IR spectra of the silver containing species show bands at 1280(vs), 1218(vs), 1155(s) and 1021(vs) cm^{-1} (compound **2**) and at 1262(vs), 1223(s), 1151(s) and 1024(s) cm^{-1} (the solid isolated from reaction *iii*), respectively, suggesting a ionic character for the triflate group.[22,34]

The ^{77}Se NMR spectra for the solid isolated from reaction (*iii*) (Scheme 1) exhibit two doublet resonances, low field shifted in comparison with the free ligand (δ –250.3 and –241.2 ppm *vs.* –294.0 ppm for the free ligand). A significant difference was also observed in the coupling constant $^1J(^{77}Se–^{31}P)$ for the free ligands ($SePPh_2Me$ and $SePPh_3$) and the silver complex species detected in solution ($[AgOTf(PPh_3)(SePPh_2Me)]$ and $[AgOTf(PPh_2Me)(SePPh_3)]$), as can be seen from the NMR data listed in Table 1.

The mass spectra (APCI+) of the solid isolated from reaction (*iii*) present peaks corresponding to the ion $[AgOTf(PPh_3)(SePPh_2Me)^+]$ [*m*/*z* 800.9(80%)] as well as the ion $[Ag(PPh_3)(SePPh_2Me)^+ + Se]$ [*m*/*z* 729.6(100%)].

Solution behaviour of the solid isolated from the reaction between $[CuNO_3(PPh_3)_2]$ and $SePPh_2Me$

Apparently, the solid isolated from reaction (*vii*) (Scheme 1) proved to have a similar behaviour in solution as it was described above for the silver species $\{[Ag(PPh_xMe_{3-x})(SePPh_yMe_{3-y})]OTf\}_n$. The ^{1}H and ^{31}P NMR spectra recorded at room temperature either in $CDCl_3$ or acetone-d_6 solution present four resonances, two of them at high field, sharp and accompanied by ^{77}Se satellites, and the other two broad, at low field. These four signals might be considered as forming two sets of resonances, similarly to the situation described before for the silver(I) complex species **3**, **3a** and **4**, **4a**. The ^{77}Se NMR spectrum presents two doublets, one of them at δ –266.3 ppm [^1J(SeP) 728.8 Hz] and the other at δ –275.2 ppm [^1J(SeP) 715.5 Hz]. These values are almost identical to those found for the free triorganophosphane selenides $SePPh_2Me$ and $SePPh_3$ (Table 1). Moreover, the ^{31}P NMR chemical shifts are similar to those observed for the species $SePPh_2Me$, $SePPh_3$ and $[CuNO_3(PPh_3)_2]$, respectively (Table 1). The fourth resonance at δ –17.4 ppm (in acetone-d_6) was tentatively assigned to $[CuNO_3(PPh_2Me)_2]$. Taking in account this similarity, we presume that even if in reaction (*vii*) an equilibrium process involving both transfer of selenium from $SePPh_2Me$ to PPh_3 and association in dimeric units can take place in a first instance, as depicted in Scheme 1, due to the high lability of the resulted copper(I) species and the overcrowded metal center, subsequent processes of dissociation/recombination occurred, resulting in $SePPh_2Me$, $SePPh_3$, $[CuNO_3(PPh_2Me)_2]$, $[CuNO_3(PPh_3)_2]$ and $[CuNO_3(PPh_3)(PPh_2Me)]$ species (Scheme 1). An evidence in this sense is also the fact that attempts to grow single-crystals of the solid isolated from this reaction resulted in the isolation of $SePPh_3$ or $[CuNO_3(PPh_3)_2]$.

Low temperature ^{31}P NMR spectra of the copper species brought no clear evidence for an equilibrium between a mixture of monomeric (**8** and **9**) and dimeric (**8a** and **9a**) species, as was described above for the silver(I) complex species **3** and **4**, respectively, but such a dimerization process can not be excluded as occurring in the first stage of the reaction. At –75 °C, the two ^{31}P resonances corresponding to the phosphines, PPh_3 and PPh_2Me, respectively, attached to copper have an aspect of multiplets. This aspect suggests the existence of a third bis(triorganophosphane)copper(I) species in solution, *i.e.* $[CuNO_3(PPh_3)(PPh_2Me)]$, and it might be determined by very close chemical shift values of the *P*Ph_3 and *P*Ph_2Me ligands in the three types of bis(triorganophosphane) copper(I) complexes and by the fact that at such low temperature

even the two phosphorus atoms in species containing the same triorganophosphanes attached to the metal center are no more equivalent (see ESI, Fig. S3†).

The room temperature ^{77}Se NMR spectrum for the solid isolated from reaction (*vii*) in Scheme 1, as well as for a reaction mixture of $[CuNO_3(PPh_3)_2]$ and $SePPh_2Me$ in a 1 : 1 molar ratio realized directly in the NMR tube, presents two doublets, one of them at δ –266.3 ppm [^1J(PSe) 728.8 Hz] and the other at δ –275.2 ppm [^1J(PSe) 715.5 Hz].

In order to bring more arguments in the favour of the dynamic processes described before, for both the silver(I) and the copper(I) species containing both P(III) and P(V) ligands, we performed further NMR experiments reacting directly in the NMR tube (*a*) a 1 : 1 reaction mixture of $SePPh_3$ and AgOTf and (*b*) a 1 : 1 reaction mixture of PPh_3 and $SePPh_2Me$. In first case the δ(^{31}P) and δ(^{77}Se) values for the P(V) species are shifted in comparison with those observed for the Ag(I) species described above, while in the second case the δ(^{31}P) and δ(^{77}Se) values are almost identical to those observed for the Cu(I) species (Table 1). Reaction (*b*) revealed that the transfer of selenium from a P(V) to a P(III) species according to eqn (1) takes place even in the absence of a metal center, as it was previously described and documented both by experimental and computational methods for few other couples of organophosphorus species of type EPR_3 and PR'_3 (E = O, S, Se).[35–37]

$$PPh_3 + SePPh_2Me \rightleftharpoons SePPh_3 + PPh_2Me \quad (1)$$

The mass spectra (ESI+) of the solid resulted from reaction (*vii*) contains peaks corresponding to the species $[CuNO_3(PPh_3)(SePPh_2Me)^+]$ (*m*/*z* 667.5, 5%), $[Cu(PPh_3)(SePPh_2Me)^+]$ (*m*/*z* 605.5, 72%) and $[CuNO_3(PPh_3)(PPh_2Me)^+]$ (*m*/*z* 588.5, 100%).

Crystal and molecular structure of compounds 6 and 7

The ORTEP-like representations for compounds **6** and **7** are depicted in Fig. 2 and Fig. 3, respectively, while relevant bond distances and angles are given in Table 2.

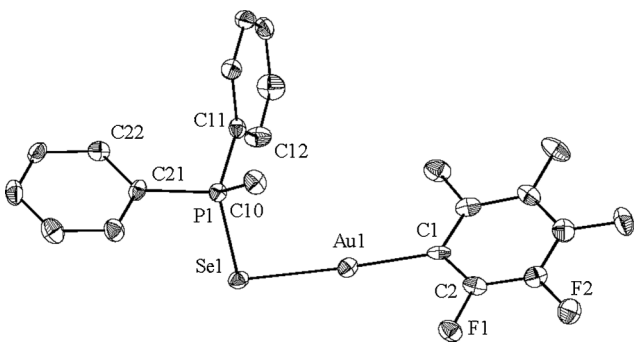

Fig. 2 ORTEP plot of $[Au(C_6F_5)(SePPh_2Me)]$ (**6**). The atoms are drawn with 50% probability ellipsoids.

The gold complexes **6** and **7** are essentially monomeric species, although in complex **6** the gold–gold distance between two neighbouring molecules is just at the limit below the sum of the van der Waals radii for gold [3.3387(7) Å *vs.* Σr_{vdW}(Au,Au) 3.40 Å[38]].

Table 2 Selected bond distances (Å) and angles (°) for compounds **6** and **7**

6		**7**	
Au1–C1	2.059(7)	Au1–C1	2.073(5)
Au1–Se1	2.4353(11)	Au1–C11	2.055(5)
Au1 ··· Au1′	3.3387(7)	Au1–C21	2.070(5)
Se1–P1	2.1769(18)	Au1–Se1	2.5128(7)
P1–C10	1.798(7)	Se1–P1	2.1787(14)
P1–C21	1.804(7)	P1–C30	1.794(5)
P1–C11	1.819(7)	P1–C31	1.811(5)
		P1–C41	1.805(5)
C1–Au1–Se1	176.72(16)	C11–Au1–Se1	174.00(14)
C1–Au1 ··· Au1′	108.06(16)	C21–Au1–Se1	92.88(13)
Se1–Au1 ··· Au1′	75.22(2)	C1–Au1–Se1	89.21(13)
P1–Se1–Au1	94.05(5)	C11–Au1–C21	89.40(19)
C10–P1–C21	106.5(3)	C11–Au1–C1	88.63(19)
C10–P1–C11	107.8(3)	C21–Au1–C1	177.63(19)
C21–P1–C11	108.3(3)	P1–Se1–Au1	102.98(4)
C10–P1–Se1	112.4(2)	C30–P1–C41	110.1(3)
C21–P1–Se1	107.9(2)	C30–P1–C31	107.5(2)
C11–P1–Se1	113.8(2)	C41–P1–C31	106.6(2)
		C30–P1–Se1	110.34(18)
		C41–P1–Se1	114.05(17)
		C31–P1–Se1	108.02(17)

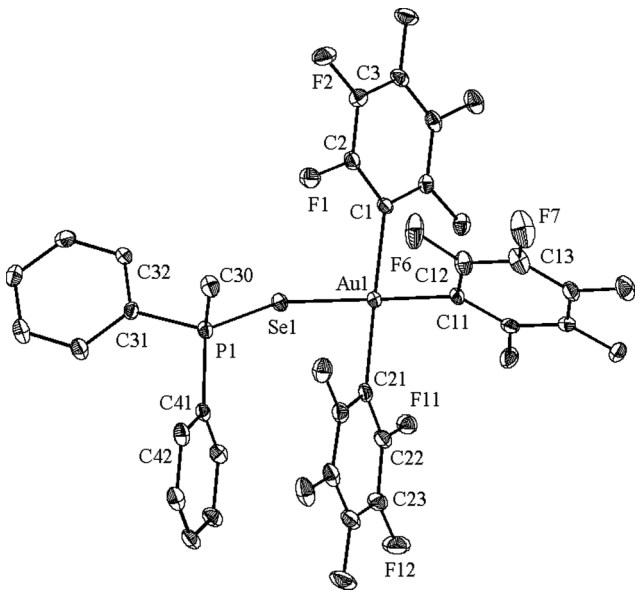

Fig. 3 ORTEP plot of $[Au(C_6F_5)_3(SePPh_2Me)]$ (**7**). The atoms are drawn with 50% probability ellipsoids.

The organophosphorus(V) ligand $SePPh_2Me$ behaves as a monometallic monoconnective moiety in both gold complexes, being attached to the metal centre through selenium. In complex **6** the coordination geometry about the gold(I) atom is linear, slightly distorted [C1–Au1–Se1 176.72(16)°].

Taking into account the weak Au ··· Au contact, a T-shaped coordination geometry can be assigned [Se1–Au1 ··· Au1′ 75.22(2)° and C1–Au1 ··· Au1′ 108.06(16)°]. In complex **7** the gold atom has a square planar geometry. The C_6F_5 group *trans* to selenium is twisted to almost 90° with respect to the other two pentafluorophenyl rings. The phosphorus atoms have tetrahedral coordination geometries in both complexes, while the selenium atoms have distorted *pseudo* tetrahedral coordination

Table 3 Luminescent spectral data for the ligand $SePPh_2Me$ and compounds **6** and **7** in solid state

Compound	λ_{max} (298 K) emission (excitation)	λ_{max} (77 K) emission (excitation)
$SePPh_2Me$	448 (398)	440 (385) 480 shoulder (385)
$[Au(C_6F_5)(SePPh_2Me)]$ (**6**)	—	500 (395)
$[Au(C_6F_5)_3(SePPh_2Me)]$ (**7**)	396, 482 (283)	360, 446 broad (310)

geometries [P1–Se1–Au1 94.05(5)° in **6** and 102.98(4)° in **7**, respectively]. The P═Se distances [P═Se 2.1769(18) Å in **6** and 2.1787(14) Å in **7**, respectively] are of similar magnitude to those found in $[Au(C_6F_5)_2\{SePPh_2CHPPh_2SeAu(C_6F_5)_3\}]$ [2.1814(8) and 2.1716(10) Å][27] or $[Au(C_6F_5)_2\{(SePPh_2)_2N\}]$ [2.1970(6) and 2.1953(7) Å],[13] but longer than in $(Se{=}PPh_2)_2NH$ [2.085(1) and 2.101(1) Å].[39]

The selenium-gold distances [2.4353(11) Å in **6** and 2.5128(7) Å in **7**, respectively], are close to those found in other gold(I) or gold(III) complexes with P–Se–Au bonds, *i.e.* 2.4352(3) Å in $[Au_2\{(SePPh_2)_2N\}(PPh_3)_2]OTf$, 2.4808(3) and 2.4832(3) Å in $[Au(C_6F_5)_2\{(SePPh_2)_2N\}]$,[13] 2.4639(4) and 2.4940(4) Å in $[Au(C_6F_5)_2\{SePPh_2CHPPh_2SeAu(C_6F_5)_3\}]$.[27]

Luminescence studies

The diffuse reflectance ultraviolet visible spectra (DRUV) were recorded for the gold complexes **6** and **7**. The spectrum of complex **6** consists of a band with two maxima at 231 and 260 nm and that of **7** of a band with a maximum at 276 nm. Both complexes are weakly emissive in the solid state, complex **6** only at 77 K and complex **7** at room temperature and at 77 K too. Complex **6** displays one emission (Table 3) at 500 nm (Fig. 4) and complex **7** shows two emissions, one at 360 and the other one, a not well resolved structured band, at about 446 nm.

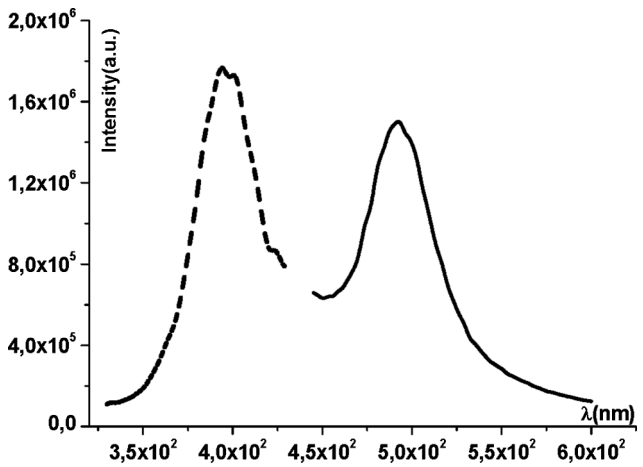

Fig. 4 Excitation (dashed line) and emission (straight line) spectrum of complex **6** at 77 K.

The ligand $SePPh_2Me$ is also emissive at room temperature and at 77 K. At room temperature it shows an emission at 448 nm and at 77 K there is a maximum at 440 nm with a shoulder at 480 nm. The emissions observed in the gold(III) derivative **7** resembles those of the ligand, then the origin of the emissions is based on intraligand transitions (IL), whereas in complex **6** with a gold(I) fragment only one emission is observed and it is shifted towards low energy, indicating that the origin of the emission is probably intraligand but modified due to the coordination to the metal and the presence of gold(I)···gold(I) interactions in the structure.

Table 4 Selected bond distances (Å) and angles (°) calculated for **3** (M = Ag) and **8** (M = Cu) at DFT level

	3[a]	**3**[b]	**8**[a]	**8**[b,c]
P1–M	2.411	2.419	2.232	2.233
Se–M	2.518	2.542	2.323	2.328
P2–Se	2.191	2.193	2.194	2.201
P2–Se–M	97.64	96.19	95.52	95.75
P1–M–Se	177.39	176.67	177.28	177.76

[a] Calculated in the gas phase. [b] Calculated in acetone (PCM-IEF). [c] P–Se distance = 2.126 Å for $SePPh_2Me$ in the gas phase.

Theoretical calculations on 3, 8, 3a, and 8a

One of the most intriguing results arising from the spectroscopic NMR measurements discussed above is the alleged tendency of both species **3** and **4** to dimerize in solution to give **3a** and **4a**, respectively. In order to ascertain the nature of such dimers, DFT calculations have been carried out on **3** and **3a**.

The optimized structure of **3** shows the silver(I) cation linearly coordinated by the triphenylphosphine and the methyldiphenylphosphine selenide (Se–Ag–P angle = 177.39°), with the P═Se bond disposed almost orthogonally to the P1–Ag–Se fragment (Table 4).

NBO charge distribution shows that the chalcogen atom features the most negative charge (Q_{Se} = –0.396 e in **3** as compared to Q_{Se} = –0.499 e in $SePPh_2Me$), while the silver atom is positively charged (Q_{Ag} = 0.373 e). In addition, the Kohn–Sham Highest Occupied Molecular Orbital (KS-HOMO) calculated for **3** shows a large contribution from the lone pair located on the selenium atom (Fig. 5), while the LUMO is mainly built up of the antibonding σ-in-nature MO of the P═Se bond. Interestingly, LUMO+1 shows a large contribution from the empty 5s orbital of the silver atom. In order to verify whether the electronic structure calculated for **3** is preserved in the solvent medium (acetone) adopted for ^{1}H-NMR measurements, the geometry optimization was also performed according to the IEF-PCM approach.

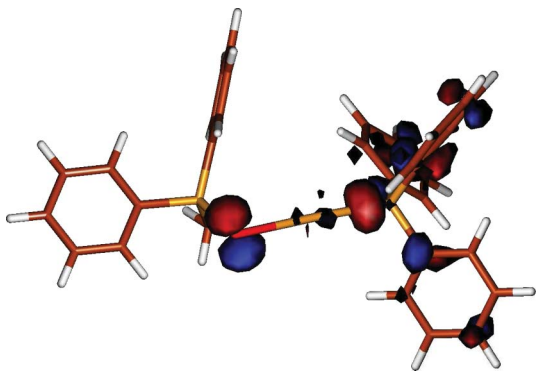

Fig. 5 KS-HOMO drawing calculated for **3** in the gas phase. Cutoff value 0.05 e.

Table 5 Selected bond distances (Å) and angles (°) calculated for **3a** at DFT level. Atom labeling as in Fig. 6

	3a[a,c]	**3a**[a,d]	**3a**[b,c]	**3a**[b,d]
P1–Ag	2.421	2.414	2.443	2.424
Se–Ag	2.534	2.535	2.585	2.561
P2–Se[e]	2.197	2.204	2.190	2.205
$Ag^A \ldots Se^{B,f}$		3.281[a]		2.998[b]
P2–Se–Ag	99.08	97.45	99.57	98.09
P1–Ag–Se	170.88	178.52	157.91	177.70

[a] Calculated in the gas phase. [b] Calculated in acetone (PCM-IEF). [c] Unit A of the dimer (See Fig. 6). [d] Unit B of the dimer (see Fig. 6). [e] P–Se distance = 2.126 Å for $SePPh_2Me$ in the gas phase. [f] Distance between the silver atoms belonging to the two interacting units A and B.

An examination of the bond lengths and angles shows only small variations as compared to the corresponding ones calculated in the gas phase (Table 4).

The nature of the KS-HOMO and the natural charge distribution (Q_{Se} = –0.463, Q_{Ag} = 0.481 e) indicate that the polarisation of the Ag–Se bond is remarkably increased (ΔQ_{Ag-Se} = 0.769 and 0.943 e in the gas phase and in acetone, respectively) and confirm the selenium atom as the most donor site.

The optimized structure of **3a** in the gas phase (Fig. 6, Table 5) shows that, in agreement with natural atomic charges and the composition of HOMO and LUMO+1, the compound is formed by a head-to-tail combination of the two molecular units by a single interaction between the selenium donor site of one unit and the Ag center of a second one (units B and A, respectively, in Fig. 6) with a Ag···Se contact of 3.281 Å (sum of van der Waals contact 3.62 Å). The triorganophosphane chalcogenide ligand, therefore, would not bridge symmetrically the two metal centres. Notably, the molecular unit whose silver atom is involved in the contact (unit A) undergoes a distortion resulting in a bending of the P–Ag–Se fragment (by about 7°) and small elongations in the P–Ag and Se–Ag bonds, by 0.010 and 0.016 Å, respectively (Tables 4 and 5). On passing from the gas phase to the acetone solution, the optimized metric parameters indicate that the interaction between the two units of **3** is strengthened. Accordingly, the

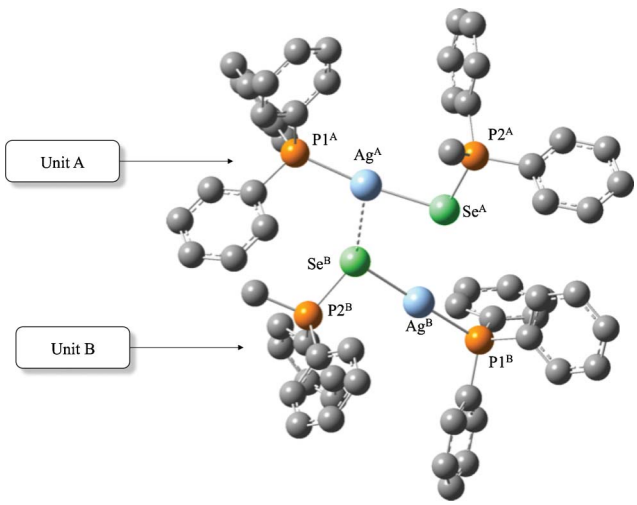

Fig. 6 Ball and stick drawing of the molecular structure of **3a** optimized at DFT level in the gas phase. Hydrogen atoms have been omitted for clarity.

Ag···Se distance between the two monomers is remarkably shortened (2.998 Å) and the distortions in the two units of **3a** with respect to the optimized structure of **3** are more pronounced, with the coordination sphere around the Ag^A ion involved into the interaction with the triorganophosphane chalcogenide ligand tending to a trigonal planar three-coordination.

The head-to-tail conformation calculated for **3a** supports the hypothesis that indeed both Ag centers could be alternatively involved in the Ag···Se contact discussed above, so that a fast equilibrium on NMR time scale between the dimer featuring the $Ag^A \cdots Se^B$ interaction and the dimer featuring the $Ag^B \cdots Se^A$ contact would justify the presence in the ^{31}P NMR spectrum at room temperature of only two ^{31}P resonances for the dimeric species.

Analogous calculations were carried out for the copper complex **8**. The complex features the copper ion dicoordinated in a linear Se–Cu–P geometry closely resembling that of the silver homologue **3** (Table 4). Also the composition of the KS-HOMO, mainly due to a lone pair localized on the selenium atom, with a minor contribution from the copper ion, is very similar to that calculated for **3**. This notwithstanding, the virtual MO's in the range LUMO-LUMO+5 (about 0.22 eV), contrary to what observed for **3**, show only very small contributions from the metal ion. This could possibly prevent those intramolecular interactions, between the Se donor atom of a unit and the metal ion of another unit, which the dimer formation is based on in the case of **3a**. Notably, the calculation including the effect of the solvent (acetone), implicitly taken into account, does not affect remarkably neither the molecular geometry (Table 4) nor the composition of the frontier KS-MO's of **8**.

An attempt to optimise a hypothetical dimer **8a** showing structural features similar to those calculated for **3a** was carried out. The optimization steps led to the elimination of PPh_2Me, with formation of a dinuclear species $[Cu_2(PPh_3)_2(SePPh_2Me)(Se)]^{2+}$, featuring a Cu–Cu bond [d(Cu–Cu) = 2.908 Å; WBI (Cu–Cu) = 0.145] and a selenide bridge between the two metal ions, which show different charges (+0.232 and +0.018 e) suggesting a mixed-valence nature for the compound. It is worth noting that copper-copper interactions of the same order of magnitude as those calculated for $[Cu_2(PPh_3)_2(SePPh_2Me)(Se)]^{2+}$ have been reported in several cases of cluster compounds featuring phosphanes and selenated ligands.[40–42] Although $[Cu_2(PPh_3)_2(SePPh_2Me)(Se)]^{2+}$ might be unstable, and possibly prelude to the formation of other species, the calculation allows confirming the instability of **8a**, in agreement with the experimental NMR data discussed before.

DFT calculations were extended to gold(I) and gold(III) complexes **6** and **7** in order to investigate their electronic structure and the spectroscopic features discussed above.

In the case of **6**, whose X-ray diffraction analysis showed Au(I)···Au(I) interactions between couples of molecular complexes, both the isolated molecular unit (**6**) and a couple of units (**6′**), kept together by the aurophilic interactions, were optimized starting from structural data. In Table 6, some selected bond distances and angles are summarised for the two optimized structures. It is remarkable that **6** and **6′** show metric parameters very close to each other, and in very good agreement with the structural data obtained by single crystal X-ray diffraction (Table 2). In particular, it should be underlined that the calculated Au···Au distance in **6′**, related to the evaluation of the aurophilic

Table 6 Selected bond distances (Å) and angles (°) calculated for **6**, **6′**, and **7** at DFT level. Atom labeling as in Fig. 2 and Fig. 3. The corresponding structural values are listed in Table 2

	6	**6′**		**7**
Au1–C1	2.029	2.031	Au1–C1	2.069
Au1–Se1	2.504	2.503	Au1–C11	2.034
Au1 ··· Au1″	—	3.360	Au1–C21	2.075
Se1–P1	2.181	2.181	Au1–Se1	2.569
P1–C10 (Me)	1.816	1.819	Se1–P1	2.192
P1–C21	1.816	1.819	P1–C30	1.813
P1–C11	1.821	1.820	P1–C31	1.820
			P1–C41	1.813
C1–Au1–Se1	178.12	179.71	C11–Au1–Se1	174.62
C1–Au1 ··· Au1′	—	89.36	C21–Au1–Se1	96.15
Se1–Au1 ··· Au1′	—	90.58	C1–Au1–Se1	86.28
P1–Se1–Au1	94.72	94.85	C11–Au1–C21	88.59
C10–P1–C21	106.13	106.62	C11–Au1–C1	88.99
C10–P1–C11	107.93	106.69	C21–Au1–C1	177.57
C21–P1–C11	106.11	107.73	P1–Se1–Au1	102.34
C10–P1–Se1	112.28	112.16	C30–P1–C41	109.56
C21–P1–Se1	108.82	108.75	C30–P1–C31	106.24
C11–P1–Se1	115.19	114.52	C41–P1–C31	107.06
			C30–P1–Se1	112.20
			C41–P1–Se1	114.55
			C31–P1–Se1	106.71

interaction, is very close to the experimental value (3.360 and 3.3387(7) Å, respectively), directly confirming the choice of the RECP adopted for the gold species.

In Fig. 7 the orbital energy diagram calculated for **6** along with the isosurfaces of selected frontier Kohn–Sham molecular orbitals, ranging between HOMO-6 (MO 100) and LUMO+9 (MO 115), are depicted. Worthy of note, gold(I) contributes with the 5*d* AO's to the highest filled orbitals (see MO's 100, 104 and 106 in Fig. 7), while the lowest unoccupied ones are mainly localised on the phenyl groups.

The pattern of molecular orbitals of **6′** derives directly from the overlap of the MO of each molecular unit. Optimized structural data and the comparison of the molecular orbitals calculated for **6** and **6′** contribute to indicate that the Au(I) ··· Au(I) interaction does not affect significantly the electronic structure of each interacting unit. Accordingly, the Wiberg bond index calculated for the Au ··· Au system (0.118) indicates a weak interaction, confirmed by a stabilisation in the electronic energy of about 6.6 kcal mol^{-1} (ΔH_f = 5.92 kcal mol^{-1} at 298 K taking into account Zero Point Energy and thermal corrections).

TD-DFT calculations were exploited to simulate the electronic absorption spectrum of the complexes in the UV-Vis region and to get a deeper insight into the emission processes. A comparison of the spectra calculated for **6** and **6′** shows that in both cases the absorption spectra in the region 230–500 nm are dominated by electronic transitions falling at about 250 nm, in very good agreement with diffuse reflectance experiments showing absorption maxima between 230 and 260 nm. Such absorption can be attributed to the vertical transitions to the singlet excited states (ES's) S38 and S39, in turn due to monoelectronic excitations having a large MLCT character (S38: MO 212 → MO 219, f = 0.084, E = 4.850 eV; S39: 205 → 214 and 203 → 213, f = 0.134, E = 4.888 eV). This notwithstanding, experimental excitation spectra recorded at 77 K for compound **6** in the solid-state (Table 3) clearly show that a weaker absorption at 395 nm is responsible for the fluorescent emission observed at 500 nm. Such an absorption,

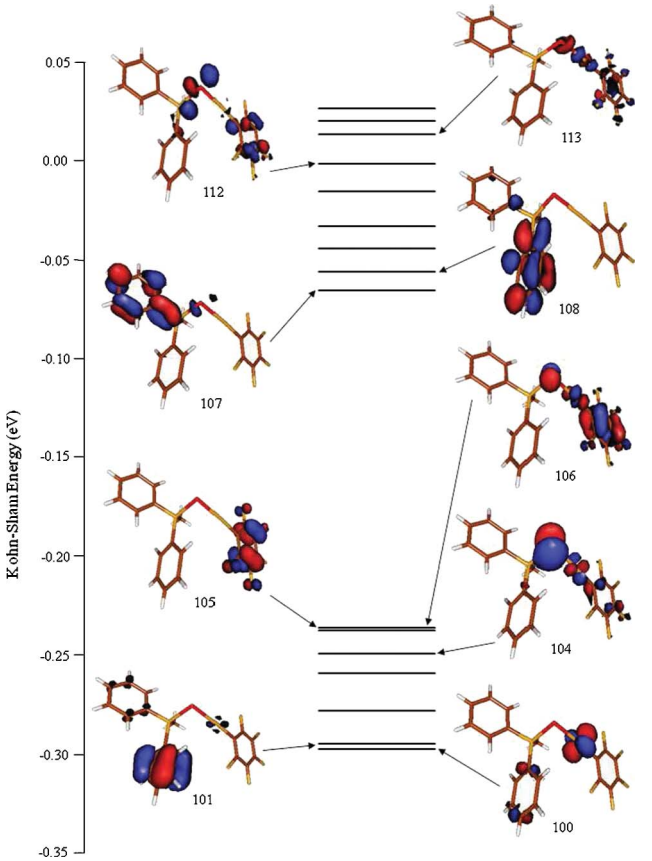

Fig. 7 Energy diagram and KS-MO isosurface drawings of the frontier orbitals calculated for **6**. HOMO = MO 106, LUMO = MO 107. Cutoff value = 0.05 e.

peculiar to **6′** and therefore directly related to the aurophilic interaction, can be envisaged in the electronic transition involving ES S3, calculated at 4.026 eV (f = 0.103), largely due to the HOMO–LUMO monoelectronic excitation (Fig. 8).

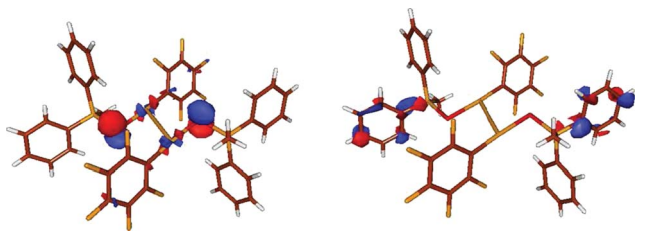

Fig. 8 KS-HOMO (left) and LUMO (right) calculated for **6′** in the gas phase. Cutoff value = 0.05 e.

TD-DFT calculations were also carried out on the complex **7**, fluorescent both at 77 K and at room temperature (Table 3), whose optimized geometry (Table 6) is in excellent agreement with the structural data (Table 2). As mentioned above, the DRUV spectrum recorded for **7** at 298 K clearly shows a structured band featuring an absorption maximum at 276 nm. The excitation spectrum at 298 K features a maximum at roughly the same energy (283 nm, Table 3).

A comparison between the experimental UV-Vis spectrum and the simulated spectrum based on TD-DFT calculations shows

that the absorption band derives from three main contributions, involving the singlet ES's S40, S47, and S59. The electronic transition featuring the highest oscillator strength is that involving S40 (5.494 eV, $f = 0.497$), largely (40%) due to a monoelectronic excitation from KS-MO 180 (corresponding to the LP localised on the chalcogen atom of the $SePPh_2Me$ ligand) to MO 189 [involving the Se atom, the π* system of one of the phenyl groups of the same ligand, and to a lesser extent a 5*d* AO of the Au(III) ion]. Therefore, the main absorption in the UV region is ILCT in nature and regards an excitation process localised on the $SePPh_2Me$ ligand, in perfect agreement with the conclusions drawn on the basis of the luminescence studies discussed above.

Conclusions

Several group 11 metal complexes ([CuCl($SePPh_2Me$)] (**1**), [AgOTf($SePPh_2Me$)] (**2**), [AuCl($SePPh_2Me$)] (**5**), [Au(C_6F_5)($SePPh_2Me$)] (**6**) and [Au(C_6F_5)$_3$($SePPh_2Me$)] (**7**) were isolated and structurally characterized in solution by multinuclear NMR spectroscopy. For the gold complexes **6** and **7** monomeric structures were determined by single-crystal X-ray diffraction, and they were further optimized by DFT calculations. In case of compound **6** weak aurophilic gold(I) $\cdots$ gold(I) contacts were also observed in the crystal.

The DRUV spectra have shown that complexes **6** and **7**, as well as the ligand $SePPh_2Me$ are emissive in the solid state, complex **6** only at 77 K and complex **7** and the free ligand both at room temperature and at 77 K. TD-DFT calculations were performed in order to investigate the electronic properties which determin the luminescence of complexes **6** and **7**, as well as of the ligand $SePPh_2Me$ in the solid state.

The products isolated from the reactions between $SePPh_2Me$ and [$CuNO_3(PPh_3)_2$] or [AgOTf(PPh_3)] prooved to have a dynamic solution behavior involving the transfer of selenium from the P(V) species $SePPh_2Me$ to the P(III) phosphane PPh_3. In case of the silver(I) species the NMR experiments brought further evidence for dimerization processes resulting in {[Ag(PPh_3)(μ-$SePPh_2Me$)]$_2$($OTf)_2$ (**3a**) and [Ag(PPh_2Me)(μ-$SePPh_3$)]$_2$($OTf)_2$ (**4a**)}, while in case of the Cu(I) species the NMR experiments suggest the formation of decomposition products, *i.e.* the copper(I) complexes [$CuNO_3(PPh_3)_2$], [$CuNO_3(PPh_2Me)_2$] and [$CuNO_3(PPh_3)(PPh_2Me)$] and the triorganophosphane selenides $SePPh_2Me$ and $SePPh_3$ in equilibrium, even if in the first stage of the reaction the formation of monomeric {[$CuNO_3(PPh_3)_2$($SePPh_2Me$)] (**8**) and [$CuNO_3(PPh_2Me)$($SePPh_3$)] (**9**)}, and dimeric {[Cu(PPh_3)(μ-$SePPh_2Me$)]$_2$($NO_3)_2$ (**8a**) and [Cu(PPh_2Me)(μ-$SePPh_3$)]$_2$($NO_3)_2$ (**9a**)} might be also envisaged.

DFT calculations are in accordance with a head-to-tail conformation for **3a**, thus supporting the hypothesis that both Ag centers in a dimeric unit could be alternatively involved in the Ag $\cdots$ Se contact so that a fast equilibrium on NMR time scale between the dimer featuring the $Ag^A \cdots Se^B$ interaction and the dimer featuring the $Ag^B \cdots Se^A$ contact takes place, in accordance with the ^{31}P NMR spectrum at room temperature. The attempt to optimize a hypothetical dimer **8a** showing structural features similar to those calculated for **3a** suggest the elimination of PPh_2Me, with formation of an unstable dinuclear species [$Cu_2(PPh_3)_2$($SePPh_2Me$)(Se)]$^{2+}$, which might prelude the further decomposition, in accordance with the NMR spectra.

Experimental

General procedures

All synthetic manipulations were carried out under argon atmosphere using Schlenk techniques. Solvents were dried and freshly distilled prior to use. The starting materials, [AuCl(tht)],[43] [Au(C_6F_5)(tht)], [Au(C_6F_5)$_3$(tht)],[44] [AgOTf(PPh_3)],[45] [$CuNO_3(PPh_3)_2$][46] and $SePPh_2Me$,[47] were prepared according to literature methods. The commercial reagents AgOTf, CuCl, $Cu(NO_3)_2$, PPh_3 and PPh_2Me were purchased from Sigma Aldrich and used without further purification. Elemental analyses were performed on a VarioEL analyser. Infrared spectra were recorded on a Jasco FT-IR machine, as KBr pellets. NMR spectra were recorded on a BRUKER Avance 300 instrument (^1H, ^{31}P and ^{77}Se) and a VARIAN GEMINI 400S instrument (^{19}F) operating at 300, 121.5, 57.2 and 376.5 MHz, respectively, in $CDCl_3$ or acetone-d_6 solutions. Chemical shifts are reported in ppm relative to TMS (^1H), trifluoracetic acid (^{19}F) and H_3PO_4 85% (^{31}P). The ^{77}Se spectra were obtained using diphenyl diselenide as external standard. Chemical shifts are reported relative to dimethyl selenide (δ 0 ppm) by assuming that the resonance of the standard is at δ 461 ppm.[48] 2D heteronuclear ^{31}P-^1H NMR correlation experiments (HMQC) were used to assign the resonances for the copper(I) and silver(I) complexes in solution. Mass spectra were recorded on an Agilent 6320 Ion Trap instrument. DRUV spectra were recorded with a UnicamUV-4 spectrophotometer equipped with a Spectralon RSA-UC-40 Labsphere integrating sphere. The intensities were recorded in Kubelka-Munk units. Steady-state photoluminescence spectra were recorded with a Jobin–Yvon Horiba Fluorolog FL-3-11 spectrometer using band pathways of 3 nm for both excitation and emission.

Synthesis of [CuCl($SePPh_2Me$)] (1). A mixture of $SePPh_2Me$ (0.115 g, 0.41 mmol) and CuCl (0.041 g, 0.41 mmol) in 20 mL anhydrous CH_2Cl_2 was stirred for 1 h at room temperature. The solvent was removed in vacuum and addition of *n*-hexane afforded the title product as a colorless solid. Yield 0.134 g (86%). Anal. Calc. for $C_{13}H_{13}ClCuPSe$ (MW 378.18): C, 41.29; H, 3.46; Found: C, 41.32; H, 3.61; ^1H NMR ($CDCl_3$): δ 2.83 (3H, d, CH_3, $^2J_{PH}$ 13.7 Hz), 7.47 (4H, m, C_6H_5-*meta*), 7.54 (2H, m, C_6H_5-*para*), 7.74 (4H, ddd, C_6H_5-*ortho*, $^3J_{PH} = 13.7$, $^3J_{HH} = 7.4$, $^4J_{HH} = 1.6$ Hz); ^{31}P NMR ($CDCl_3$): δ 21.17 (s, $^1J_{SeP}$ 598.5 Hz). ESI+ MS *m*/*z*(%): 720.8 (10) [($CuSePPh_2Me)_2Cl^+$], 622.8 (100) [Cu($SePPh_2Me)_2^+$ + H]; ESI– MS *m*/*z*(%):613.8 (100) [(Cu(PPh_2Me) ($SePPh_2Me)_2Cl_2^-$].

Synthesis of [AgOTf($SePPh_2Me$)] (2). A mixture of $SePPh_2Me$ (0.092 g, 0.33 mmol) and AgOTf (0.085 g, 0.33.mmol) in 20 mL anhydrous CH_2Cl_2 was stirred for 2 h at room temperature. The solvent was removed in vacuum and addition of *n*-hexane afforded the title product as a colorless powder. Yield 0.127 g (72%). Anal. Calc. for $C_{14}H_{13}AgF_3O_3PSSe$ (MW 536.11): C, 31.36; H, 2.44. Found: C, 31.29; H, 2.42. ^1H NMR (acetone-d_6): δ 2.95 (3H, d, CH_3, $^2J_{PH}$ 13.8 Hz), 7.64 (4H, dt, PC_6H_5-*meta*, $^3J_{HH}$ 7.8, $^4J_{HH}$ 3.6 Hz), 7.74 (2H, dt, PC_6H_5-*para*, $^3J_{HH}$ 7.5, $^4J_{HH}$ 2.1 Hz), 7.92 (4H, ddd, PC_6H_5-*ortho*, $^3J_{HH}$ 7.2, $^4J_{HH}$ 1.4, $^3J_{PH}$ 14.3 Hz). ^{31}P NMR (acetone-d_6): δ 27.7 (s, $^1J_{SeP}$ 535.4 Hz). ^{19}F NMR (acetone-d_6): δ –79.8 (s, OTf). ESI+ MS *m*/*z*(%): 559.4 (100) [M^+ + Na]; ESI– MS

m/z(%): 406.7 (100) [$Ag(OTf)_2^-$]. IR (ν, cm^{-1}): 1280(vs), 1218(vs), 1155(s) and 1021(vs).

Reaction between [AgOTf(PPh$_3$)] and SePPh$_2$Me. A mixture of [AgOTf(PPh$_3$)] (0.332 g, 0.64.mmol) and SePPh$_2$Me (0.179 g, 0.64 mmol) was stirred for 2 h at room temperature in 20 mL acetone and then worked up as described for compound **1**. A colorless powder was finally isolated. Yield 0.347 g (68%). Anal. Calc. for $C_{32}H_{28}AgF_3O_3P_2SSe$ (MW 798.40): C, 48.14; H, 3.53. Found: C, 48.22; H, 3.42. ^{1}H, ^{13}C, ^{31}P, ^{19}F and ^{77}Se NMR spectra evidence the presence of two sets of resonances which can be assigned to the species [AgOTf(PPh$_3$)(SePPh$_2$Me)] (**3**) and [Ag(PPh$_3$)(μ-SePPh$_2$Me)]$_2$(OTf)$_2$ (**3a**), and [AgOTf(PPh$_2$Me)(SePPh$_3$)] (**4**) and [Ag(PPh$_2$Me)(μ-SePPh$_3$)]$_2$(OTf)$_2$ (**4a**). **3**/**3a**: ^{1}H NMR (acetone-d_6, 293 K): δ 2.60 (3H, d, SePCH_3, $^2J_{PH}$ 13.6 Hz), 7.29–7.48 (15H, m, P*Ph*$_3$ *ortho+meta+para*) 7.48–7.53 (6H, m, P*Ph*$_2$Me *meta+para*), 7.81 (4H, dd, P*Ph*$_2$Me *ortho*, $^3J_{HH}$ 7.7, $^3J_{PH}$ 14.1 Hz). ^{31}P NMR (acetone-d_6, 293 K): δ 10.5 (s, br., *P*Ph$_3$), 25.8 (s, Se*P*Ph$_2$Me, $^1J_{SeP}$ 595.4, $^1J_{PC(Me)}$ 52.7, $^1J_{PC(Ph)}$ 75.4 Hz). ^{77}Se (acetone-d_6, 293 K): δ –250.3 (d, Ag*Se*PPh$_2$Me, $^1J_{SeP}$ 595.7 Hz). ^{19}F NMR (acetone-d_6, 293 K): δ –78.5 (s, OTf). ^{31}P NMR (acetone-d_6, 213 K): δ 8.61 (**3**, d, Ag*P*Ph$_3$, $^1J_{107Ag-31P}$ 618.9, $^1J_{109Ag-31P}$ 539.6 Hz), 9.64 (**3a**, d, Ag*P*Ph$_3$, $^1J_{107Ag-31P}$ 526.3, $^1J_{109Ag-31P}$ 460.8 Hz), 26.4 (s, AgSe*P*Ph$_2$Me, $^1J_{PSe}$ 576.5 Hz). ^{77}Se (acetone-d_6, 243 K): δ 259.1 (d, Ag*Se*PPh$_2$Me, $^1J_{PSe}$ 584.6 Hz). **4**/**4a**: ^{1}H NMR (acetone-d_6, 293 K): δ 1.85 (3H, d, CH_3, $^2J_{PH}$ 5.9 Hz), 7.48–7.53 (m, 10H, P*Ph*$_2$Me *ortho+meta+para* + 9H, SeP*Ph*$_3$*meta+para*), 7.66 (4H, dd, P*Ph*$_2$Me *ortho*, $^3J_{HH}$ 7.8, $^3J_{PH}$ 13.6 Hz). ^{31}P NMR (acetone-d_6, 293 K): δ –7.3 (s, br., Ag*P*Ph$_2$Me), 33.6 (s, AgSe*P*Ph$_3$, $^1J_{SeP}$ 625.0, $^1J_{PC(Me)}$ 52.7, $^1J_{PC(Ph)}$ 77.4 Hz). ^{77}Se (acetone-d_6, 293 K): δ –241.2 (d, Ag*Se*PPh$_3$, $^1J_{SeP}$ 626.7 Hz). ^{19}F NMR (acetone-d_6, 293 K): δ –78.7 (s, br., OTf). ^{31}P NMR (acetone-d_6, 213 K): δ –8.48 (d, br., Ag*P*Ph$_2$Me, $^1J_{AgP}$ 594.8 Hz), 32.5 (s, br., **4** + **4a**, AgSe*P*Ph$_3$, $^1J_{SeP}$ 616 Hz). MS (APCI+) *m/z*(%): 800.9 (80) [AgOTf(PPh$_3$)(SePPh$_2$Me)$^+$], 729.6 (100) [Ag(PPh$_3$)(SePPh$_2$Me)$^+$ + Se]. IR (ν, cm^{-1}): 1262 (vs), 1223(s), 1151(s) and 1024(s).

Preparation of [AuCl(SePPh$_2$Me)] (5). A mixture of SePPh$_2$Me (0.049 g, 0.18 mmol) and [AuCl(tht)] (0.056 g, 0.18 mmol) in 20 mL anhydrous CH_2Cl_2 was stirred for 30 min. at room temperature. The solvent was removed in vacuum and then the oily product was treated with *n*-hexane. A brown oily product was obtained. Yield: 0.052 g (58%). Anal. Calc. for $C_{13}H_{13}AuClPSe$ (MW 511.60): C, 30.52; H, 2.56; Found: C, 30.42; H, 2.61; ^{1}H NMR ($CDCl_3$): δ 2.61 (3H, d, CH_3, $^2J_{PH}$ 13.6 Hz), 7.55 (4H, m, PC$_6H_5$-*meta*), 7.63 (2H, t, PC$_6H_5$-*para*, $^3J_{HH}$ 5.48 Hz), 7.79 (4H, dd, PC$_6H_5$-*ortho*, $^3J_{HH}$ 7.3, $^3J_{PH}$ 14.2 Hz). ^{31}P NMR ($CDCl_3$): δ 23.1 (s, $^1J_{PC}$ 75.8, $^1J_{SeP}$ 544.8 Hz).

Preparation of [Au(C$_6$F$_5$)(SePPh$_2$Me)] (6). **6** was prepared similarly to **5** from SePPh$_2$Me (0.202 g, 0.72 mmol) and [(C$_6$F$_5$)Au(tht)] (0.327 g, 0.72 mmol) in 40 mL anhydrous CH_2Cl_2, as a microcrystalline pale yellow powder. Yield: 0.302 g, (65%). Anal. Calc. for $C_{19}H_{13}AuF_5PSe$ (MW 643.20): C, 35.48; H, 2.04. Found: C, 35.63; H, 2.11. ^{1}H NMR ($CDCl_3$): δ 2.68 (3H, d, CH_3, $^2J_{PH}$ 13.5 Hz), 7.55 (4H, dt, PC$_6H_5$-*meta*, $^3J_{HH}$ 7.6, $^4J_{PH}$ 3.2 Hz), 7.63 (2H, dt, PC$_6H_5$-*para*, $^3J_{HH}$ 7.2, $^4J_{HH}$ 2.1 Hz), 7.71 (4H, dd, PC$_6H_5$-*ortho*, $^3J_{HH}$ 7.4, $^3J_{PH}$ 14.2 Hz). ^{31}P NMR ($CDCl_3$): δ 24.2 (s, $^1J_{SeP}$ 556.5, $^1J_{PC(Ph)}$ 76.1, $^1J_{PC(Me)}$ 50.8 Hz). ^{19}F NMR ($CDCl_3$): δ –162.73 (m, AuC$_6F_5$-*meta*), –160.14 (t, AuC$_6F_5$-*para*, $^2J_{FF}$ 20.2 Hz), –116.32 (m, AuC$_6F_5$-*ortho*).

Preparation of [Au(C$_6$F$_5$)$_3$(SePPh$_2$Me)] (7). **7** was prepared similarly to **5** and **6** from SePPh$_2$Me (0.233 g, 0.83 mmol) and [(C$_6$F$_5$)$_3$Au(tht)] (0.656 g, 0.83 mmol) in 20 mL anhydrous CH_2Cl_2, as a colorless powder. Yield 0.621 g (76%). Anal. Calc. for $C_{31}H_{13}AuF_{15}PSe$ (MW 977.31): C, 38.10; H, 1.34. Found: C, 38.18; H, 1.41. ^{1}H NMR ($CDCl_3$): δ 2.66 (3H, d, CH_3, $^2J_{PH}$ 13.5 Hz), 7.51–7.56 (8H, m, PC$_6H_5$-*ortho+meta*, 7.62–7.66 (2H, m, PC$_6H_5$-*para*); ^{31}P NMR ($CDCl_3$): δ 26.05 (s, $^1J_{SeP}$ 553, $^1J_{PC(Ph)}$ 76.0, $^1J_{PC(Me)}$ 50.0 Hz). ^{19}F NMR ($CDCl_3$): δ –161.34 (2F, m, AuC$_6F_5$-*meta*), –160.95 (4F, m, AuC$_6F_5$-*meta*), –157.3 (1F, t, AuC$_6F_5$-*para*, $^2J_{FF}$ 20.0 Hz), –157.16 (2F, t, AuC$_6F_5$-*para*, $^2J_{FF}$ 20 Hz), –122.22 (2F, m, AuC$_6F_5$-*ortho*), –119.78 (4F, m, AuC$_6F_5$-*ortho*).

Reaction between [CuNO$_3$(PPh$_3$)$_2$] and SePPh$_2$Me. A mixture of SePPh$_2$Me (0.117 g, 0.42 mmol) and CuNO$_3$(PPh$_3$)$_2$ (0.272 g, 0.42 mmol) was stirred for 2 h at room temperature in 30 mL anhydrous CH_2Cl_2 and then worked up as described for compound **1**. A colorless powder was finally isolated. Yield 0.255 g (66%). Anal. Calc. for $C_{49}H_{43}CuNO_3P_3Se$ (MW 929.30): C, 63.33; H, 4.66; N, 1.51. Found: C, 63.27; H, 4.61; N, 1.54. ^{1}H NMR (acetone-d_6, 293 K): δ 1.6 (3H, d, CuPPh$_2$*Me*, $^2J_{PH}$ = 4.0 Hz), 2.51 (3H, d, CuSePPh$_2$*Me*, $^2J_{PH}$ = 13.4 Hz), 7.19–7.44 (m, 30H, CuP*Ph*$_3$-*ortho+meta+para* + 10H CuP*Ph*$_2$Me-*meta+para*), 7.53 (m, 9H CuSeP*Ph*$_3$-*meta+para* + 6H CuSeP*Ph*$_2$Me-*meta+para*), 7.77 (4H, dd, CuSeP*Ph*$_3$-*ortho*, $^3J_{PH}$ = 13.2, $^3J_{HH}$ = 7.4 Hz), 7.94 (4H, ddd, CuSeP*Ph*$_2$Me-*ortho*, $^3J_{PH}$ = 13.4, $^3J_{HH}$ = 7.0, $^4J_{HH}$ = 1.6 Hz). ^{31}P NMR (acetone-d_6, 293 K): δ –18.8 (s, br., Cu*P*Ph$_2$Me), –2.25 (s, br., Cu*P*Ph$_3$), 23.6 (s, Se*P*Ph$_2$Me, $^1J_{SeP}$ 731.8, $^1J_{PC}$ 74 Hz), 35.2 (s, Se*P*Ph$_3$, $^1J_{SeP}$ 746.3 Hz). ^{31}P NMR (acetone-d_6, 198 K): δ –18.8 (m, Cu*P*Ph$_2$Me), –1.27 (d, Cu*P*Ph$_3$, $^2J_{PP}$ 83.5 Hz), 24.5 (s, Se*P*Ph$_2$Me, $^1J_{SeP}$ 719.7, $^1J_{PC(Ph)}$ 73.0, $^1J_{PC(Me)}$ 53.0 Hz), 35.3 (s, Se*P*Ph$_3$, $^1J_{SeP}$ 736.8, $^1J_{PC}$ 76.8 Hz). ^{1}H NMR ($CDCl_3$, 293 K): δ 1.59 (3H, d, CuPPh$_2$*Me*, $^2J_{PH}$ = 2.54 Hz), 2.46 (3H, d, CuSePPh$_2$*Me*, $^2J_{PH}$ = 13.3 Hz), 7.35–7.14 (m, 15H, CuP*Ph*$_3$-*ortho+meta+para* + 6H, CuP*Ph*$_2$Me-*meta+para*), 7.47 (m, 9H, CuSeP*Ph*$_3$-*meta+para* + 6H, CuSeP*Ph*$_2$Me-*meta+para*), 7.75 (6H, dd, CuSeP*Ph*$_3$-*ortho*, $^3J_{PH}$ = 13.6, $^3J_{HH}$ = 6.8 Hz), 7.83 (4H ddd, CuSeP*Ph*$_2$Me-*ortho*, $^3J_{PH}$ = 13.5, $^3J_{HH}$ = 7.3, $^4J_{HH}$ = 1.5 Hz). ^{31}P NMR ($CDCl_3$, 293 K): δ –17.4 (s, br., Cu*P*Ph$_2$Me), –1.2 (s, br., Cu*P*Ph$_3$), 23.3 (s, Se*P*Ph$_2$Me, $^1J_{SeP}$ 715.3, $^1J_{PC}$ 74 Hz), 35.4 (s, Se*P*Ph$_3$, $^1J_{SeP}$ 728.0 Hz). ^{31}P NMR ($CDCl_3$, 198 K): δ –17.3 (m, Cu*P*Ph$_2$Me), –0.75 (m, Cu*P*Ph$_3$), 23.8 (s, Se*P*Ph$_2$Me, $^1J_{SeP}$ 692.0 Hz), 35.4 (s, Se*P*Ph$_3$, $^1J_{SeP}$ 709, $^1J_{PC}$ 77.2 Hz). ^{77}Se NMR ($CDCl_3$, 293 K): δ –266.3 (d, Cu*Se*PPh$_2$Me, $^1J_{PSe}$ = 728.8 Hz), –275.2 (d, Cu*Se*PPh$_3$, $^1J_{PSe}$ = 715.5 Hz). MS (ESI+) *m/z*(%): 667.5 (5), [CuNO$_3$(PPh$_3$)(SePPh$_2$Me)$^+$] 605.5 (72) [Cu(PPh$_3$)(SePPh$_2$Me)$^+$], 588.5 (100) [CuNO$_3$(PPh$_3$)(PPh$_2$Me)$^+$].

Crystal structures

Single-crystals of compounds **6** (pale yellow) and **7** (colorless) were grown by slow diffusion in CH_2Cl_2/*n*-hexane (1/5, v/v) systems. Details of the crystal structure determination and refinement for compounds **6** and **7** are given in Table 7.

Data were measured using Mo-Kα radiation (λ = 0.71073) on a Xcalibur Oxford Diffraction diffractometer. Absorption corrections were based on multiple scans (program SADABS).[49] The structures were solved by Direct Methods, and refined by

Table 7 Crystalllographic data for compounds **6** and **7**

	6	**7**
Empirical formula	$C_{19}H_{13}AuF_5PSe$	$C_{31}H_{13}AuF_{15}PSe$
M	643.19	977.31
T	100(2)	100(2)
Crystal system	Monoclinic	Monoclinic
Space group	*P*21/c	*P*21/c
a/Å	9.0631(18)	10.848(2)
b/Å	21.657(4)	20.482(4)
c/Å	9.6803(19)	13.523(3)
α (°)	90	90
β (°)	96.97(3)	97.75(3)
γ (°)	90	90
V/Å^3	1886.0(6)	2977.3(10)
Absorption correction	Multi-Scan[49]	Multi-Scan[49]
μ(Mo-Kα)/mm^{-1}	9.863	6.336
R_1 [$I > 2\sigma(I)$]	0.0383	0.0310
wR_2	0.0736	0.0655
GOF on F^2	1.321	1.083

full-matrix least-squares on F^2 (SHELXL-97).[50] All non-hydrogen atoms were refined anisotropically. H atoms were included using a riding model. The drawings were created with the Diamond program.[51] CCDC reference numbers 827811 (**6**) and 827812 (**7**)†.

DFT calculations

Quantum-chemical calculations based on the Density Functional Theory (DFT)[52] were carried out on the ligand $SePPh_2Me$, the compounds **3** and **8** and their dimeric forms **3a** and **8a** (Scheme 1), respectively, the Au(I) species **6** and the compound **6′** (consisting of two units of **6** interacting through a Au···Au interaction), and the Au(III) complex **7** by adopting the mPW1PW functional[53] and using the commercially available suite of programs Gaussian09.[54] Schäfer, Horn, and Ahlrichs double-zeta plus polarization all-electron basis sets (BS's)[55] were used for C, H, F and P, while LanL08 BS's with relativistic effective core potentials (RECP) were adopted for the heavier Se and metal (Cu, Ag, Au) species, providing in addition d-type and f-type, respectively, polarization functions.[56] The geometry optimizations (with tight cutoff values on forces and step size) were performed without introducing any structural simplification or symmetry restrain. In the case of **3a**, the geometry was optimized in the presence of the solvent (acetone), implicitly taken into account by means of the Polarizable Continuum Model approach in its integral equation formalism variant (IEF-PCM), which describes the cavity of the solute within the reaction field through a set of overlapping spheres.[57] In all cases, a pruned (99,590) grid was adopted (Ultrafine option) in order to avoid imaginary frequencies. A full Natural Bond Orbital analysis[58] was carried out at the optimized geometries using the NBO module version 3.1.[59] Time-dependent (TD) DFT calculations were carried out on the gold complexes **6** (100 states), **6′** (50 states), and **7** (75 states) in order to understand their absorption/emission spectroscopic features. The programs GaussView and Molden 4.8 were used to investigate the charge distributions and MO's shapes,[60] while GaussSum 2.6 [61] was exploited for investigating the nature of the electronic transitions calculated at TD-DFT level.

Acknowledgements

Financial support from the Ministry of Education and Research of Romania (CNCSIS, Research Project ID-2404/2008) and the Ministerio de Ciencia e Innovación (CTQ2010-20500-C02-01) is greatly appreciated. A. Pop thanks the European Social Fund for a Scholarship (Education and Training Program 2008-2013, POSDRU/6/1.5/S/3). We warmly acknowledge Prof. Konstantin Karaghiosoff for helpful discussions.

References

1 W. E. Van Zyl, J. M. Lopez-de-Luzuriaga and J. P. Fackler, Jr., *J. Mol. Struct.*, 2000, **516**, 99.
2 M. Preisenberger, A. Bauer, A. Schier and H. Schmidbaur, *J. Chem. Soc., Dalton Trans.*, 1997, 4753.
3 I. Haiduc, G. Mezei, R. Micu-Semeniuc, F. T. Edelmann and A. Fischer, *Z. Anorg. Allg. Chem.*, 2006, **632**, 295.
4 M. Shafaei-Fallah, C. E. Anson, D. Fenske and A. Rothenberger, *Dalton Trans.*, 2005, 2300.
5 D. Fenske, A. Rothenberger and M. Shafaei-Fallah, *Z. Anorg. Allg. Chem.*, 2004, **630**, 943.
6 P. G. Jones, A. Blaschette, J. Lautner and C. Thone, *Z. Anorg. Allg. Chem.*, 1997, **623**, 775.
7 C. Wolper, S. R. Pinol, S. D. Ibanez, M. Freytag, P. G. Jones and A. Blaschette, *Z. Anorg. Allg. Chem.*, 2008, **634**, 1506.
8 V. Latorre, P. G. Jones, O. Moers and A. Blaschette, *Z. Anorg. Allg. Chem.*, 2003, **629**, 1943.
9 E.-M. Zerbe, P. G. Jones and A. Blaschette, *Z. Anorg. Allg. Chem.*, 2007, **633**, 1265.
10 P. G. Jones, D. Henschel, A. Weitze and A. Blaschette, *Z. Anorg. Allg. Chem.*, 1994, **620**, 1514.
11 I. Haiduc, in A. B. P. Lever, (Ed.), *Comprehensive Coordination Chemistry II. From Biology to Nanotechnology*, Vol. 1, Elsevier, 2003, p. 323.
12 J. D. E. T. Wilton-Ely, A. Schier and H. Schmidbaur, *Inorg. Chem.*, 2001, **40**, 4656.
13 S. Canales, O. Crespo, C. M. Gimeno, P. G. Jones, A. Laguna, A. Silvestru and C. Silvestru, *Inorg. Chim. Acta*, 2003, **347**, 16.
14 H. Liu, N. A. G. Bandeira, M. J. Calhorda, M. G. B. Drew, V. Felix, J. Novosad, F. Fabrizi de Biani and P. Zanello, *J. Organomet. Chem.*, 2004, **689**, 2808.
15 H. Rudler, B. Denise, J. Ribeiro Gregorio and J. Vaissermann, *Chem. Commun.*, 1997, 2299.
16 G. L. Abbati, M. C. Aragoni, M. Arca, M. B. Carrea, F. A. Devillanova, A. Garau, F. Isaia, V. Lippolis, M. Marcelli, C. Silvestru and G. Verani, *Eur. J. Inorg. Chem.*, 2005, 589.
17 A. M. Z. Slawin and M. B. Smith, *New J. Chem.*, 1999, **23**, 777.
18 A. M. Z. Slawin, M. B. Smith and J. D. Woollins, *J. Chem. Soc., Dalton Trans.*, 1998, 1537.
19 C. Daniliuc, C. Druckenbrodt, C. G. Hrib, F. Ruthe, A. Blaschette, P. G. Jones and W.-W. du Mont, *Chem. Commun.*, 2007, 2060.
20 G. Pilloni, B. Longato, G. Bandoli and B. Corain, *J. Chem. Soc., Dalton Trans.*, 1997, 819.
21 G. Pilloni, B. Longato and G. Bandoli, *Inorg. Chim. Acta*, 2000, **298**, 251.
22 S. Canales, O. Crespo, M. Concepcion Gimeno, P. G. Jones and A. Laguna, *J. Organomet. Chem.*, 2000, **613**, 50.
23 T. S. Rimple, A. Castineiras and P. Turner, *Inorg. Chem.*, 2003, **42**, 4731.
24 J. R. Black and W. Levason, *J. Chem. Soc., Dalton Trans.*, 1994, 3225.
25 T. S. Lobana, R. Mahajan and A. Castineiras, *Transition Met. Chem.*, 2001, **26**, 440.
26 T. S. Lobana, P. Mahajan, A. S. Pannu, G. Hundal and R. J. Butcher, *J. Coord. Chem.*, 2007, **60**, 733.
27 S. Canales, O. Crespo, M. C. Gimeno, P. G. Jones and A. Laguna, *Z. Naturforsch., B: Chem. Sci.*, 2007, **62**, 407.
28 E. L. Muetterties and C. W. Alegranti, *J. Am. Chem. Soc.*, 1972, **94**, 6386.
29 P. F. Barron, J. C. Dyason, P. C. Healy, L. M. Engelhardt, B. W. Skelton and A. H. White, *J. Chem. Soc., Dalton Trans.*, 1986, 1965.

30 A. Caballero, A. Guerrero, F. A. Jalon, B. R. Manzano, R. M. Claramunt, M. D. Santa Maria, C. Escolastico and J. Elguero, *Inorg. Chim. Acta*, 2003, **347**, 168.
31 A. Ilie, C. I. Rat, S. Scheutzow, C. Kiske, K. Lux, T. M. Klapotke, C. Silvestru and K. Karaghiosoff, *Inorg. Chem.*, 2011, **50**, 2675.
32 M. Barrow, H.-B. Burgi, M. Camalli, F. Caruso, E. Fischer, L. M. Venanzi and L. Zambonelli, *Inorg. Chem.*, 1983, **22**, 2356.
33 H. Friebolin, *Basic and Two Dimensional NMR Spectroscopy*, VCH, Weinheim, 1992.
34 S. J. Angus-Dunne, L. E. P. Lee Chin, R. C. Burns and G. A. Lawrance, *Transition Met. Chem.*, 2006, **31**, 268.
35 M. Kullberg and J. Stawinski, *J. Organomet. Chem.*, 2005, **690**, 2571, and references cited therein.
36 S. Trofimenko, A. L. Rheingold and C. D. Incarvito, *Angew. Chem., Int. Ed.*, 2003, **42**, 3506.
37 M. Bollmark and J. Stawinski, *Chem. Commun.*, 2001, 771.
38 J. Emsley, *Die Elemente*, Walter de Gruyter, Berlin, 1994.
39 P. Battacharyya, A. M. Z. Slawin, V. Garcia-Montalvo, J. Novosad, J. D. Woolins, R. A. Toscano and G. Espinosa-Perez, *Chem. Ber.*, 1996, **129**, 919.
40 O. Fuhr, A. Meredith and D. Fenske, *J. Chem. Soc., Dalton Trans.*, 2002, 4091.
41 C. Nitschke, D. Fenske and J. F. Corrigan, *Inorg. Chem.*, 2006, **45**, 9394.
42 A. I. Wallbank, A. Borecki, N. J. Taylor and J. F. Corrigan, *Organometallics*, 2005, **24**, 788.
43 R. Uson, A. Laguna and M. Laguna, *Inorg. Synth.*, 1989, **26**, 85.
44 E. J. Fernandez, P. G. Jones, A. Laguna, J. M. Lopez-de-Luzuriaga, M. Monge, M. E. Olmos and R. C. Puelles, *J. Chem. Soc., Chem. Commun.*, 1976, 353.
45 M. Bardaj, O. Crespo, A. Laguna and A. K. Fischer, *Inorg. Chim. Acta*, 2000, **304**, 7.
46 F. H. Jardine, A. G. Vohra and F. J. Young, *J. Inorg. Nucl. Chem.*, 1971, **33**, 2941.
47 F. Montilla, A. Galindo, V. Rosa and T. Aviles, *Dalton Trans.*, 2004, 2588.
48 P. N. Jayaram, G. Roy and G. Mugesh, *J. Chem. Sci.*, 2008, **120**, 143.
49 G. M. Sheldrick, *SADABS Program for area detector adsorption correction*, Institute for Inorganic Chemistry, University of Göttingen, Germany, 1996.
50 G. M. Sheldrick, *SHELX-97*, Universität Göttingen, Germany, 1997.
51 *DIAMOND—Visual Crystal Structure Information System*, CRYSTAL IMPACT, Postfach 1251, D-53002 Bonn, Germany, 2001.
52 C. J. Cramer, *Essentials of Computational Chemistry*, Chapter 8, 2nd Ed., Wiley, Chechester (England), 2004.
53 C. Adamo and V. Barone, *J. Chem. Phys.*, 1998, **108**, 664.
54 *Gaussian 09*, Revision A.1, M. J. Frisch, G. W. Trucks, H. B. Schlegel, G. E. Scuseria, M. A. Robb, J. R. Cheeseman, G. Scalmani, V. Barone, B. Mennucci, G. A. Petersson, H. Nakatsuji, M. Caricato, X. Li, H. P. Hratchian, A. F. Izmaylov, J. Bloino, G. Zheng, J. L. Sonnenberg, M. Hada, M. Ehara, K. Toyota, R. Fukuda, J. Hasegawa, M. Ishida, T. Nakajima, Y. Honda, O. Kitao, H. Nakai, T. Vreven, J. A. Montgomery, Jr., J. E. Peralta, F. Ogliaro, M. Bearpark, J. J. Heyd, E. Brothers, K. N. Kudin, V. N. Staroverov, R. Kobayashi, J. Normand, K. Raghavachari, A. Rendell, J. C. Burant, S. S. Iyengar, J. Tomasi, M. Cossi, N. Rega, J. M. Millam, M. Klene, J. E. Knox, J. B. Cross, V. Bakken, C. Adamo, J. Jaramillo, R. Gomperts, R. E. Stratmann, O. Yazyev, A. J. Austin, R. Cammi, C. Pomelli, J. W. Ochterski, R. L. Martin, K. Morokuma, V. G. Zakrzewski, G. A. Voth, P. Salvador, J. J. Dannenberg, S. Dapprich, A. D. Daniels, Ö. Farkas, J. B. Foresman, J. V. Ortiz, J. Cioslowski and D. J. Fox, Gaussian Inc, Wallingford CT, 2009.
55 A. Schäfer, H. Horn and R. Ahlrichs, *J. Chem. Phys.*, 1992, **97**, 2571.
56 L. E. Roy, P. J. Hay and R. L. Martin, *J. Chem. Theory Comput.*, 2008, **4**, 1029.
57 J. Tomasi, B. Mennucci, C. Cappelli and S. Corni, *Chem. Rev.*, 2005, **105**, 2999.
58 A. E. Reed, L. A. Curtiss and F. Weinhold, *Chem. Rev.*, 1988, **88**, 899, and references therein.
59 *NBO Version 3.1, E. D. Glendening, A. E. Reed, J. E. Carpenter, and F. Weinhold.*
60 G. Schaftenaar and J. H. Noordik, *J. Comput.-Aided Mol. Des.*, 2000, **14**, 123.
61 N. M. O'Boyle, A. L. Tenderholt and K. M. Langner, *J. Comput. Chem.*, 2008, **29**, 839.

